

KM3NeT sensitivity to a flux of down-going nuclearites

Alice Păun,^{a,b,*} Gabriela Păvălaș^a and Vlad Popa^a on behalf of the KM3NeT Collaboration

^a*Institute of Space Science,
Atomiștilor 409, Măgurele, Romania*

^b*University of Bucharest – Faculty of Physics,
Atomiștilor 405, Măgurele, Romania*

E-mail: alice.paun@spacescience.ro

Nuclearites are hypothetical, massive particles of Strange Quark Matter (SQM) introduced by E. Witten in 1984. They are composed of approximately equal quantities of up, down, and strange quarks. Due to the third quark flavor component which leads to a total energy lower than in the case of nuclear matter, SQM could represent the ground state of Quantum Chromodynamics (QCD). The detection and characterization of nuclearites could also bring important contributions to the Dark Matter physics. KM3NeT is a network of deep-sea neutrino telescopes placed in the Mediterranean Sea, optimized for the search for high-energy cosmic neutrinos (KM3NeT/ARCA) and the study of neutrino properties with atmospheric neutrinos (KM3NeT/ORCA). Nuclearites above a mass threshold of 10^{13} GeV/ c^2 having velocities of approximately 250 km/s could reach the ground and interact in the detector through elastic collisions. A fraction of the energy generated in these collisions is dissipated as visible blackbody radiation. A customized Monte Carlo (MC) program was used to simulate the propagation and the signal of nuclearites inside the KM3NeT detector. The background considered for this study is represented by the ^{40}K decay, which is added during the filtering stage of the MC output, and by the simulated atmospheric muons. The analysis uses selection cuts in order to remove the main background of atmospheric muons and to estimate the sensitivity of the detector. Preliminary results on the sensitivity of the KM3NeT neutrino telescope to a flux of massive down-going nuclearites will be presented.

38th International Cosmic Ray Conference (ICRC2023)
26 July - 3 August, 2023
Nagoya, Japan



*Speaker

1. Introduction

Nuclearites, or Strange Quark Matter (SQM) aggregates, are hypothetical slow (~ 250 km/s at the entry in the atmosphere), massive, and compact particles introduced by E. Witten in early 1984 [1, 2]. The theory assumes that they are composed of three quark flavors (up, down, and strange) [2] and their structure is similar to that of an atom (nucleus and electronic shell) [2, 3]. Due to the third quark flavor component which leads to a total energy lower than in the case of nuclear matter [4, 5], the strange quark matter could be the ground state of the Quantum Chromodynamics (QCD) [1, 6, 7]. The confirmation of this hypothesis could bring an important contribution to fundamental physics.

The detection of nuclearites could be done through the blackbody radiation emitted in the visible spectrum as a result of the elastic collision with the atoms of the transparent media along their paths [2]. Considering this feature, nuclearites could be detected in large-volume underwater neutrino telescopes.

As the Coulomb repulsion does not allow direct nuclear interactions with atoms due to the electronic shell, nuclearites interact predominantly through elastic and quasi-elastic collisions. The energy emitted in these collisions overheats the medium along the particle trajectory. In transparent media, such as water, a part of this energy is dissipated as blackbody radiation in the visible spectrum, denoted luminous efficiency ($\eta \approx 3 \cdot 10^{-5}$) [2]. The energy loss follows Equation 1 [2]:

$$\frac{dE}{dx} = -\sigma \rho v^2, \quad (1)$$

where σ is the cross-section of the nuclearite, ρ is the medium density and v is the velocity of the particle. The velocity follows the Equation 2 [2]:

$$v(L) = v_0 \cdot e^{-\frac{\sigma}{M_N} \cdot \int_0^L \rho dx}, \quad (2)$$

where L is the length of the path, v_0 is the nuclearite velocity at the entry into the atmosphere and M_N is the nuclearite mass.

The cross-section of the nuclearites can be computed as a function of their mass (see Equation 3) [2]:

$$\sigma = \begin{cases} \pi \left(\frac{3M_N}{4\pi\rho_N} \right)^{\frac{2}{3}} \text{ cm}^2, & \text{for } M_N \geq 8.4 \cdot 10^{14} \text{ GeV} \\ \pi \cdot 10^{-16} \text{ cm}^2, & \text{for } M_N < 8.4 \cdot 10^{14} \text{ GeV} \end{cases} \quad (3)$$

where $\rho_N = 3.6 \cdot 10^{14} \text{ g/cm}^3$ is the density of the nuclearite.

The number of emitted photons per unit length is given by Equation 4 [2]:

$$\frac{dN_\gamma}{dx} = \eta \frac{dE/dx}{\langle E_\gamma \rangle}, \quad (4)$$

where $\langle E_\gamma \rangle \approx 3.14 \text{ eV}$ is the average energy of the photons emitted in the visible spectrum.

A very important aspect regarding the detection of nuclearites with such instruments is the constant background present at the detectors level [10]. The main background component for nuclearites at the detector depth is represented by atmospheric muons [8, 10], while the ^{40}K decay and the bioluminescence (in the case of ORCA) also play an important role [8, 9].

2. The KM3NeT sensitivity to nuclearites

The KM3NeT detector is composed of two configurations of photomultiplier (PMT) arrays, currently under construction in the Mediterranean Sea: ARCA (Astroparticle Research with Cosmics in the Abyss) and ORCA (Oscillation Research with Cosmics in the Abyss). KM3NeT/ARCA will have two building blocks with 115 detection units (DUs) each, with the goal of identifying the high-energy cosmic neutrino sources. KM3NeT/ORCA will have a single, and more compact building block with 115 DUs. Its goal is to find a solution for the neutrino mass hierarchy problem. The two arrays are similar, both comprising DUs with 18 digital optical modules (DOMs) and 31 PMTs per DOM. However, the main differences are in the distribution of the detection instruments, size, and depth.

Massive particles of SQM that propagate through water could be detected by the light emitted from the blackbody radiation generated at the interaction of the particle with the atoms and molecules of the medium.

In this analysis, nuclearite events were generated with a dedicated MC program [11] for a mass range of $M_N \in [3 \cdot 10^{13} - 10^{17}] \text{ GeV}/c^2$ for both of the KM3NeT configurations. The initial flux of SQM particles considered in the simulation is 1000 events per mass. The MC production was carried out using the GRID platform hosted by the IN2P3/CNRS Computing Center.

In [11] it is shown that nuclearites that are propagated through underwater detectors, like KM3NeT or ANTARES, induce events that could be easily recognized by the large hits number and signal duration ($> 1 \text{ ms}$).

In order to determine the feasibility of nuclearite detection with the KM3NeT underwater detector, the sensitivity of the detection instrument must be computed. This study takes into account simulated background noise due to the atmospheric muon flux at the depth of the detector. The background due to the ^{40}K decay in sea water is also added in the processing step.

The strategy of the analysis aims to first establish the best selection criteria that could separate the nuclearite signal from other background noise present in the seawater that could be recorded by the detection instruments and then to determine the sensitivity of the detector to a flux of nuclearites. In order to make the selection, the relevant selection criteria are chosen and then a series of cuts are evaluated to establish the optimal ones for the considered selection criteria. This is done by minimizing the rejection factor (MRF method) [13]. The MRF technique consists of varying the cuts in small steps in order to obtain optimum cuts for the discrimination variables, that are leading to the maximization of the sensitivity results.

A KM3NeT analysis software has been used to separate the nuclearite signal from the background noise. The package includes a program that filters the MC data by using two muon trigger algorithms which are based on the maximum time-correlated light that can be observed on any

DOM within the detector and the maximum time-correlated light that can be observed on any PMT within the detector under a track assumption.

As it was mentioned before, in the case of nuclearite detection the flux of down-going atmospheric muons is a crucial background component. To separate the muons signal from the nuclearite MC data, a MC atmospheric muon production (10 TeV and 50 TeV energy thresholds for ARCA and 1 GeV for ORCA) obtained with the MUPAGE software [12] was used.

Nuclearites are slow particles compared to atmospheric muons, which are relativistic. Thus, due to the large signal duration and strong luminous signal relative to muons, a single nuclearite can give rise to many triggered events. This nuclearite particularity can be observed also in Figure 1 and Figure 2 where it can clearly be seen that the distribution of the triggered events per timeslice in the case of nuclearites has a relatively wide range. A timeslice is a collection of all frames of the detector that correspond to the same timestamp.

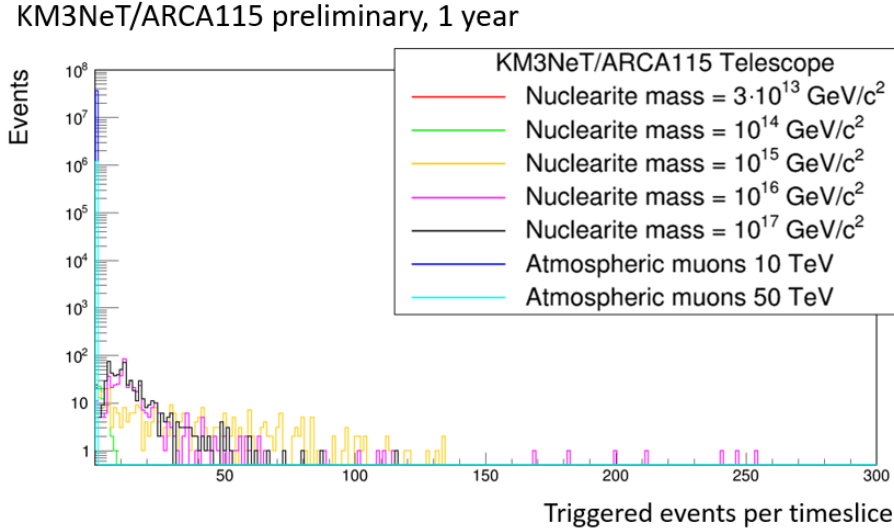


Figure 1: Distribution of the number of triggered events per timeslice in the case of KM3NeT/ARCA115.

Comparing Figures 1 and 2, one can observe there is an important difference regarding the multiplicity distribution between ARCA and ORCA. There are ORCA events with multiplicity values larger than for ARCA, particularly for smaller masses, as the triggered events are also more numerous. The characteristics mentioned above are a consequence of the higher PMT density of ORCA and are summarized in the first half of Tables 1 and 2.

After the filtering process, the next step is event selection. Three selection variables were considered for the nuclearite events: the triggered hits (an L1 trigger that occurs when at least two hits are detected in a given time interval at the same DOM), the snapshot hits (the raw hit information on all hits in a time interval larger than the triggered event) and the snapshot duration (the time interval between the first and the last snapshot hit: $[T_{MinTrig} - T_{Extra}, T_{MaxTrig} + T_{Extra}]$, where $T_{MinTrig}$ is the time of the first triggered hit, $T_{MaxTrig}$ is the time of the last triggered hit and T_{Extra} is the time offset for snapshot). The most promising discrimination variable to reduce atmospheric muon background is the snapshot duration (see Figure 3), as a larger number of nuclearite events

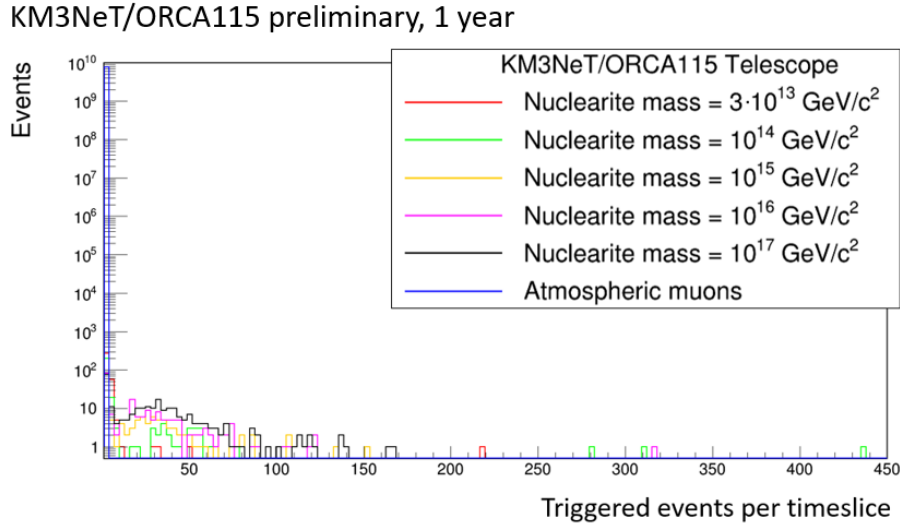


Figure 2: Distribution of the number of triggered events per timeslice in the case of KM3NeT/ORCA115.

pass this cut.

In the event selection of the data, it is very important to apply appropriate cuts in order to discriminate better between the noise and relevant signal. In this matter, for the optimization of the cuts, the atmospheric muon distributions were fitted and extrapolated by using a normalized form of the Gaussian function in the case of the snapshot duration variable for KM3NeT/ARCA and an exponential function for KM3NeT/ORCA. The optimal cuts for the two configurations are illustrated in Figure 3 by the red dashed lines. In this figure, the snapshot duration distribution is represented versus the MC events, considering the largest snapshot within the MC event.

Nuclearite mass (GeV/c ²)	Remaining MC events	Remaining triggered events	Snapshot duration (MC) > 19000 ns
$3 \cdot 10^{13}$	21	21	0
10^{14}	94	223	71
10^{15}	344	11737	319
10^{16}	468	8645	430
10^{17}	609	8276	577
Atmospheric muons	9060195 (10 TeV) 3261452 (50 TeV)	9060195 (10 TeV) 3261452 (50 TeV)	$4.92443 \cdot 10^{-6}$

Table 1: Output of the optimal cuts on the discrimination variables for KM3NeT/ARCA.

Nuclearite mass (GeV/c ²)	Remaining MC events	Remaining triggered events	Snapshot duration (MC) > 6700 ns
$3 \cdot 10^{13}$	339	1062	1
10^{14}	252	2992	29
10^{15}	154	2832	62
10^{16}	200	4651	101
10^{17}	258	7792	144
Atmospheric muons	103935982 (1 GeV)	103941853 (1 GeV)	$3.91748 \cdot 10^{-5}$

Table 2: Output of the optimal cuts on the discrimination variables for KM3NeT/ORCA.

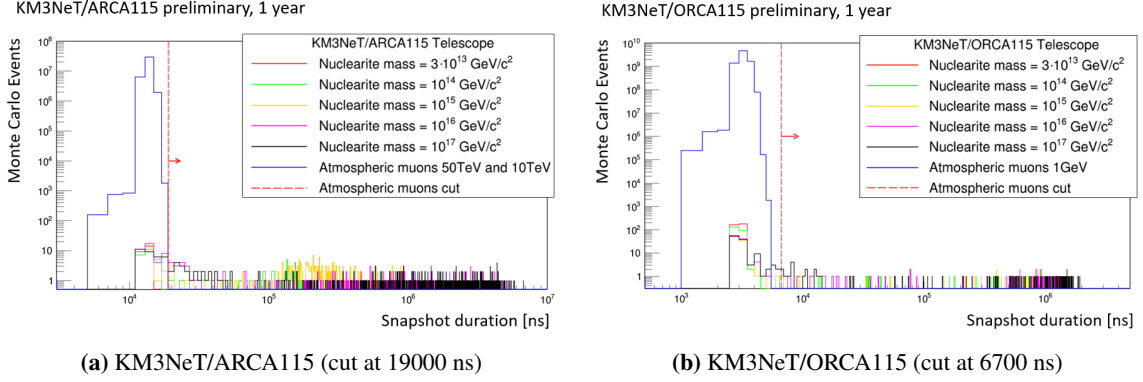


Figure 3: Distribution of the snapshot duration for MC events, considering the largest snapshot from the MC event. The optimal cut is represented by the red dashed line.

After the evaluation of the cuts, the acceptance and sensitivity of KM3NeT/ARCA and KM3NeT/ORCA to a flux of down-going nuclearites were computed and the sensitivities were compared to the upper limits obtained for MACRO [14], SLIM [15] and ANTARES (839 days of 2009-2017) [16]. The sensitivities at 90% C.L were computed by using the Feldman-Cousins formula [17] (Equation 5), considering nuclearite events with a Poisson distribution.

$$\phi_{90} = \frac{\overline{\mu}_{90}}{A \cdot T}, \quad (5)$$

where $\overline{\mu}_{90}$ was determined from the expected background using the extrapolation of the atmospheric muon distribution, T corresponds to 1 year of live time, and A is the effective acceptance of the detector (see relation 6) [17]:

$$A = \frac{S \cdot N_{nucl}}{N_{sim}}, \quad (6)$$

where S is the area of the simulation hemisphere and $\frac{N_{nucl}}{N_{sim}}$ is the ratio of the number of nuclearite events that passed the selection cuts to the number of simulated events. The results for KM3NeT/ORCA115 and KM3NeT/ARCA230 are presented in Figure 4.

The results regarding the optimized cuts for ARCA and ORCA applied to the MC data for the snapshot duration variable are listed in Table 3 and 4 together with the background, MRF values and the sensitivity of the KM3NeT detector to massive nuclearites.

Nuclearite mass (GeV/c ²)	Remaining MC events	Remaining triggered events	Background	MRF	Sensitivity 1yr (cm ⁻² sr ⁻¹ s ⁻¹)
10 ¹⁴	71	109	4.92443 · 10 ⁻⁶	0.0343732	2.0856 · 10 ⁻¹⁷
10 ¹⁵	319	3698	4.92443 · 10 ⁻⁶	0.00765047	4.642 · 10 ⁻¹⁸
10 ¹⁶	430	2410	4.92443 · 10 ⁻⁶	0.00567558	3.4437 · 10 ⁻¹⁸
10 ¹⁷	577	2450	4.92443 · 10 ⁻⁶	0.00422964	2.5664 · 10 ⁻¹⁸

Table 3: Output of the applied cut (19000 ns) on snapshot duration variable and the sensitivity estimation for KM3NeT/ARCA115 configuration to a flux of massive down-going nuclearites.

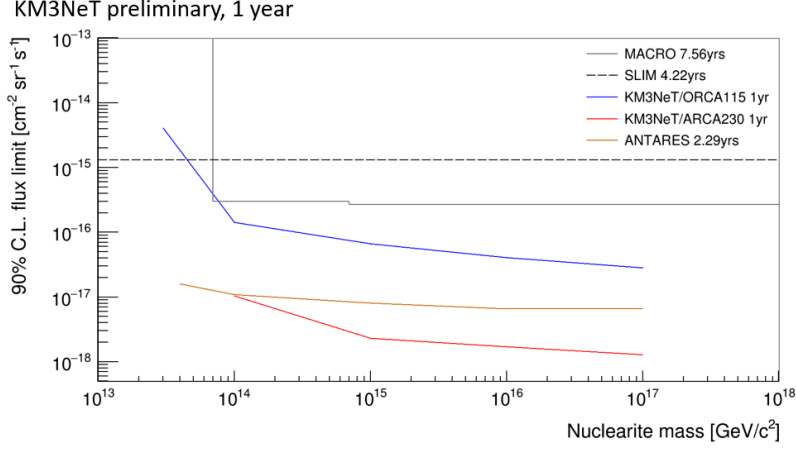


Figure 4: Preliminary sensitivities of ARCA and ORCA to a nuclearite flux compared to MACRO [14], SLIM [15], and ANTARES [16] upper limits.

Nuclearite mass (GeV/c ²)	Remaining MC events	Remaining triggered events	Background	MRF	Sensitivity 1yr (cm ⁻² sr ⁻¹ s ⁻¹)
3 · 10 ¹³	1	2	3.91748 · 10 ⁻⁵	2.44003	4.10061 · 10 ⁻¹⁵
10 ¹⁴	29	377	3.91748 · 10 ⁻⁵	0.084139	1.414 · 10 ⁻¹⁶
10 ¹⁵	62	391	3.91748 · 10 ⁻⁵	0.0393553	6.61388 · 10 ⁻¹⁷
10 ¹⁶	101	650	3.91748 · 10 ⁻⁵	0.0241587	4.06 · 10 ⁻¹⁷
10 ¹⁷	144	939	3.91748 · 10 ⁻⁵	0.0169447	2.84764 · 10 ⁻¹⁷

Table 4: Output of the applied cut (6700 ns) on snapshot duration variable and the sensitivity estimation for KM3NeT/ORCA115 configuration to a flux of massive down-going nuclearites.

3. Conclusions

The background noise is an important aspect in the detection of nuclearites with an underwater neutrino telescope. The nuclearite signal is influenced mainly by the continuous atmospheric muon flux, but also by the luminous signal produced by the decay process of ⁴⁰K always present in seawater. The signal produced by the bioluminescent organisms in the Mediterranean Sea also affects the signal of interest, but it was not considered in this analysis.

The preliminary sensitivity of KM3NeT/ARCA, determined for a flux of massive down-going nuclearites at 90% C.L. is comparable to and could improve the ANTARES upper limits obtained in [16] for 839 days of 2009-2017 data. The estimated sensitivity for KM3NeT/ORCA includes also the lightest simulated nuclearites, but is poorer than the sensitivity of KM3NeT/ARCA and ANTARES. At this point in the analysis, we can say that KM3NeT/ARCA configuration presents better characteristics for the detection and characterization of these exotic particles.

References

- [1] E. Witten (1984) Cosmic separation of phases. Physical Review D 30, 272-285, doi:10.1103/PhysRevD.30.272

- [2] A. De Rujula, S. L. Glashow (1984) Nuclearites – a novel form of cosmic radiation. *Letters to Nature* 312, 734–737, doi:10.1038/312734a0
- [3] D. Bakari (2000) Magnetic monopoles, nuclearites, Q-balls: a qualitative picture. e-Print: hep-ex/0004019 [hep-ex], doi:10.48550/arXiv.hep-ex/0004019
- [4] J. Madsen (1999) Physics and Astrophysics of Strange Quark Matter. *Lect.Notes Phys.* 516, 162-203, e-Print: astro-ph/9809032 [astro-ph], doi:10.1007/BFb0107314
- [5] F. Weber (2008) Strange Quark Matter and Compact Stars. *Progress in Particle and Nuclear Physics* 54, 193-288, doi:10.1016/j.pnpnp.2004.07.001
- [6] A. R. Bodmer (1971) Collapsed nuclei. *Physical Review D* 4, 1601-1606, doi: 10.1103/PhysRevD.4.1601
- [7] H. Terazawa (1989) Super-Hypernuclei in the Quark-Shell Model. *J. Phys. Soc. Japan* 58, 3555-3563, doi:10.1143/JPSJ.58.3555
- [8] Jannik Hofstadt (2017) Measuring the neutrino mass hierarchy with the future Km3NeT/ORCA detector. PhD Thesis, Friedrich-Alexander-Universität Erlangen-Nürnberg (FAU)
- [9] J. Reubelt (2019) Hardware studies, in-situ prototype calibration and data analysis of the novel multi-PMT digital optical module for the KM3NeT neutrino telescope. PhD Thesis, Friedrich-Alexander-Universität Erlangen-Nürnberg (FAU)
- [10] C. Kopper (2010) Performance Studies of the KM3NeT Neutrino Telescope. PhD Thesis, Friedrich-Alexander-Universität Erlangen-Nürnberg (FAU)
- [11] A. M. Paun for the KM3NeT Collaboration (2021) Search for nuclearites with the KM3NeT detector. *Journal of Instrumentation* 16 C09026, doi:10.1088/1748-0221/16/09/C09026
- [12] G. Carminati, M. Bazzotti, S. Biagi, S. Cecchini, T. Chiarusi et al. (2009) MUPAGE: a fast atmospheric MUon GEnerator for neutrino telescopes based on PArametric formulas. *Proceeding of the 31st ICRC*, doi:10.48550/arXiv.0907.5563
- [13] G. C. Hill, K. Rawlins (2003) Unbiased cut selection for optimal upper limits in neutrino detectors: the model rejection potential technique. *Astropart. Phys.* 19, 3, 393-402, doi:10.1016/S0927-6505(02)00240-2
- [14] M. Ambrosio et al., MACRO Collaboration (2000) Nuclearite search with the MACRO detector at Gran Sasso. *Eur. Phys. J. C* 13, 453–458, doi:10.1007/s100520000142
- [15] S. Cecchini, M. Cozzi, D. Di Ferdinando et al. (2008) Results of the search for strange quark matter and Q-balls with the SLIM experiment. *Eur. Phys. J. C* 57, 525–533, doi:10.1140/epjc/s10052-008-0747-7
- [16] A. Albert et al., ANTARES Collaboration (2023) Limits on the nuclearite flux using the ANTARES neutrino telescope. *JCAP* 01, 012, doi:10.1088/1475-7516/2023/01/012
- [17] G. J. Feldman, R. D. Cousins (1998) Unified approach to the classical statistical analysis of small signals. *Phys. Rev. D* 57, 3873, doi:10.1103/PhysRevD.57.3873

Full Authors List: The KM3NeT Collaboration

S. Aiello^a, A. Albert^{b,cd}, S. Alves Garre^c, Z. Aly^d, A. Ambrosone^{f,e}, F. Ameli^g, M. Andre^h, E. Androutsouⁱ, M. Anguita^j, L. Aphecetche^k, M. Ardid^l, S. Ardid^l, H. Atmani^m, J. Aublinⁿ, L. Bailly-Salins^o, Z. Bardačová^{q,p}, B. Baretⁿ, A. Bariego-Quintana^c, S. Basegmez du Pree^r, Y. Becheriniⁿ, M. Bendahman^{m,n}, F. Benfenati^{t,s}, M. Benhassi^{u,e}, D. M. Benoit^v, E. Berbee^r, V. Bertin^d, S. Biagi^w, M. Boettcher^x, D. Bonanno^w, J. Boumaaza^m, M. Bouta^y, M. Bouwhuis^r, C. Bozza^{z,e}, R. M. Bozza^{f,e}, H. Brânzaș^{aa}, F. Bretaudeau^k, R. Bruijn^{ab,r}, J. Brunner^d, R. Bruno^a, E. Buis^{ac,r}, R. Buompane^{u,e}, J. Busto^d, B. Caiffi^{ad}, D. Calvo^c, S. Champion^{g,ae}, A. Capone^{g,ae}, F. Carenini^{t,s}, V. Carretero^c, T. Cartraudⁿ, P. Castaldi^{af,s}, V. Cecchini^c, S. Celli^{g,ae}, L. Cerisy^d, M. Chabab^{ag}, M. Chadolias^{ah}, A. Chen^{ai}, S. Cherubini^{aj,w}, T. Chiarusi^s, M. Circella^{ak}, R. Cocimano^w, J. A. B. Coelhoⁿ, A. Coleiroⁿ, R. Coniglione^w, P. Coyle^d, A. Creusotⁿ, A. Cruz^{al}, G. Cuttone^w, R. Dallier^k, Y. Darras^{ah}, A. De Benedittis^e, B. De Martino^d, V. Decoene^k, R. Del Burgo^e, U. M. Di Cerbo^e, L. S. Di Mauro^w, I. Di Palma^{g,ae}, A. F. Díaz^j, C. Díaz^j, D. Diego-Tortosa^w, C. Distefano^w, A. Domi^{ah}, C. Donzau^d, D. Dornic^d, M. Dörr^{am}, E. Drakopoulouⁱ, D. Drouhin^{b,cd}, R. Dvornický^q, T. Eberl^{ah}, E. Eckerová^{q,p}, A. Eddymaoui^m, T. van Eeden^r, M. Effⁿ, D. van Eijk^r, I. El Bojaddaini^y, S. El Hedriⁿ, A. Enzenhöfer^d, G. Ferrara^w, M. D. Filipović^{an}, F. Filippini^{t,s}, D. Franciotti^w, L. A. Fusco^{z,e}, J. Gabriel^{ao}, S. Gagliardini^g, T. Gal^{ah}, J. García Méndez^l, A. Garcia Soto^c, C. Gatius Oliver^r, N. Geißelbrecht^{ah}, H. Ghaddari^y, L. Gialanella^u, B. K. Gibson^v, E. Giorgio^w, I. Goosⁿ, D. Goupilliere^o, S. R. Gozzini^c, R. Gracia^{ah}, K. Graf^{ah}, C. Guidi^{ap,ad}, B. Guillon^o, M. Gutiérrez^{aq}, H. van Haren^{ar}, A. Heijboer^r, A. Hekalo^{am}, L. Hennig^{ah}, J. J. Hernández-Rey^c, F. Huang^d, W. Idrissi Ibsalih^e, G. Illuminati^s, C. W. James^{al}, M. de Jong^{as,r}, P. de Jong^{ab,r}, B. J. Jung^r, P. Kalacznyński^{at,be}, O. Kalekin^{ah}, U. F. Katz^{ah}, N. R. Khan Chowdhury^c, A. Khatun^q, G. Kistauri^{av,au}, C. Kopper^{ah}, A. Kouchner^{aw,n}, V. Kulikovskiy^{ad}, R. Kvatadze^{av}, M. Labalme^o, R. Lahmann^{ah}, G. Larosa^w, C. Lasteria^d, A. Lazo^c, S. Le Stum^d, G. Lehaut^o, E. Leonora^a, N. Lessing^c, G. Levi^{t,s}, M. Lindsey Clarkⁿ, F. Longhitano^q, J. Majumdar^r, L. Malerba^{ad}, F. Mamedov^p, J. Mańczak^c, A. Manfreda^e, M. Marconi^{ap,ad}, A. Margiotta^{t,s}, A. Marinelli^{e,f}, C. Markouⁱ, L. Martin^k, J. A. Martínez-Mora^l, F. Marzaioli^{u,e}, M. Mastrodicasa^{ae,g}, S. Mastroianni^e, S. Micciché^w, G. Miele^{f,e}, P. Migliozzi^e, E. Migneco^w, M. L. Mitsou^e, C. M. Mollo^e, L. Morales-Gallegos^{u,e}, C. Morley-Wong^{al}, A. Moussa^y, I. Mozun Mateo^{ay,ax}, R. Muller^r, M. R. Musone^{eu}, M. Musumeci^w, L. Nautar^r, S. Navas^{aq}, A. Nayerhoda^{ak}, C. A. Nicolau^g, B. Nkosi^{ai}, B. Ó Fearraigh^{ab,r}, V. Oliviero^{f,e}, A. Orlando^w, E. Oukacha^u, D. Paesani^w, J. Palacios González^c, G. Papalashvili^{au}, V. Parisi^{ap,ad}, E. J. Pastor Gomez^c, A. M. Păun^{aa}, G. E. Pávlaš^{aa}, S. Peña Martínezⁿ, M. Perrin-Terrin^d, J. Perronnel^o, V. Pestel^{ay}, R. Pestesⁿ, P. Piattelli^w, C. Poirè^{z,e}, V. Popa^{aa}, T. Pradier^b, S. Pulvirenti^w, G. Quémener^o, C. Quiroz^l, U. Rahaman^c, N. Randazzo^{aa}, R. Randriatoamanana^k, S. Razzaque^{az}, I. C. Rea^e, D. Real^c, S. Reck^{ah}, G. Riccobene^w, J. Robinson^x, A. Romanov^{ap,ad}, A. Šaina^c, F. Salesa Greus^c, D. F. E. Samtleben^{as,r}, A. Sánchez Losa^{c,ak}, S. Sanfilippo^w, M. Sanguineti^{ap,ad}, C. Santonastaso^{ba,e}, D. Santonocito^w, P. Sapienza^w, J. Schnabel^{ah}, J. Schumann^{ah}, H. M. Schutte^x, J. Seneca^r, N. Sennan^y, B. Setter^{ah}, I. Sgura^{ak}, R. Shanidze^{au}, Y. Shitov^p, F. Šimković^q, A. Simonelli^e, A. Sinopoulou^a, M. V. Smirnov^{ah}, B. Spisso^e, M. Spurio^{t,s}, D. Stavropoulosⁱ, I. Štekl^p, M. Taiuti^{ap,ad}, Y. Tayalati^m, H. Tadjiti^{ad}, H. Thiersen^x, I. Tosta e Melo^{aj}, B. Trocméⁿ, V. Tsourapisⁱ, E. Tzamaridou^{ak}, A. Vacheret^o, V. Valsecchi^w, V. Van Elewyck^{aw,n}, G. Vannoye^d, G. Vasileiadis^{bb}, F. Vazquez de Sola^r, C. Verilhac^u, A. Veutro^{g,ae}, S. Viola^w, D. Vivolo^{u,e}, J. Wilms^{bc}, E. de Wolf^{ab,r}, H. Yepes-Ramirez^l, G. Zarpapisiⁱ, S. Zavatarelli^{ad}, A. Zegarelli^{g,ae}, D. Zito^w, J. D. Zornoza^c, J. Zúñiga^c, and N. Zywucka^x.

^aINFN, Sezione di Catania, Via Santa Sofia 64, Catania, 95123 Italy

^bUniversité de Strasbourg, CNRS, IPHC UMR 7178, F-67000 Strasbourg, France

^cIFIC - Instituto de Física Corpuscular (CSIC - Universitat de València), c/Catedrático José Beltrán, 2, 46980 Paterna, Valencia, Spain

^dAix Marseille Univ, CNRS/IN2P3, CPPM, Marseille, France

^eINFN, Sezione di Napoli, Complesso Universitario di Monte S. Angelo, Via Cintia ed. G, Napoli, 80126 Italy

^fUniversità di Napoli "Federico II", Dip. Scienze Fisiche "E. Pancini", Complesso Universitario di Monte S. Angelo, Via Cintia ed. G, Napoli, 80126 Italy

^gINFN, Sezione di Roma, Piazzale Aldo Moro 2, Roma, 00185 Italy

^hUniversitat Politècnica de Catalunya, Laboratori d'Aplicacions Bioacústiques, Centre Tecnològic de Vilanova i la Geltrú, Avda. Rambla Exposició, s/n, Vilanova i la Geltrú, 08800 Spain

ⁱNCSR Demokritos, Institute of Nuclear and Particle Physics, Ag. Paraskevi Attikis, Athens, 15310 Greece

^jUniversity of Granada, Dept. of Computer Architecture and Technology/CITIC, 18071 Granada, Spain

^kSubatech, IMT Atlantique, IN2P3-CNRS, Université de Nantes, 4 rue Alfred Kastler - La Chantrerie, Nantes, BP 20722 44307 France

^lUniversitat Politècnica de València, Instituto de Investigación para la Gestión Integrada de las Zonas Costeras, C/Paranimf, 1, Gandia, 46730 Spain

^mUniversity Mohammed V in Rabat, Faculty of Sciences, 4 av. Ibn Battouta, B.P. 1014, R.P. 10000 Rabat, Morocco

ⁿUniversité Paris Cité, CNRS, Astroparticule et Cosmologie, F-75013 Paris, France

^oLPC CAEN, Normandie Univ, ENSICAEN, UNICAEN, CNRS/IN2P3, 6 boulevard Maréchal Juin, Caen, 14050 France

^pCzech Technical University in Prague, Institute of Experimental and Applied Physics, Husova 240/5, Prague, 110 00 Czech Republic

^qComenius University in Bratislava, Department of Nuclear Physics and Biophysics, Mlynska dolina F1, Bratislava, 842 48 Slovak Republic

^rNikhef, National Institute for Subatomic Physics, PO Box 41882, Amsterdam, 1009 DB Netherlands

^sINFN, Sezione di Bologna, v.le C. Berti-Pichat, 6/2, Bologna, 40127 Italy

^tUniversità di Bologna, Dipartimento di Fisica e Astronomia, v.le C. Berti-Pichat, 6/2, Bologna, 40127 Italy

^uUniversità degli Studi della Campania "Luigi Vanvitelli", Dipartimento di Matematica e Fisica, viale Lincoln 5, Caserta, 81100 Italy

^vE. A. Milne Centre for Astrophysics, University of Hull, Hull, HU6 7RX, United Kingdom

- ^wINFN, Laboratori Nazionali del Sud, Via S. Sofia 62, Catania, 95123 Italy
- ^xNorth-West University, Centre for Space Research, Private Bag X6001, Potchefstroom, 2520 South Africa
- ^yUniversity Mohammed I, Faculty of Sciences, BV Mohammed VI, B.P. 717, R.P. 60000 Oujda, Morocco
- ^zUniversità di Salerno e INFN Gruppo Collegato di Salerno, Dipartimento di Fisica, Via Giovanni Paolo II 132, Fisciano, 84084 Italy
- ^{aa}ISS, Atomistilor 409, Măgurele, RO-077125 Romania
- ^{ab}University of Amsterdam, Institute of Physics/IHEF, PO Box 94216, Amsterdam, 1090 GE Netherlands
- ^{ac}TNO, Technical Sciences, PO Box 155, Delft, 2600 AD Netherlands
- ^{ad}INFN, Sezione di Genova, Via Dodecaneso 33, Genova, 16146 Italy
- ^{ae}Università La Sapienza, Dipartimento di Fisica, Piazzale Aldo Moro 2, Roma, 00185 Italy
- ^{af}Università di Bologna, Dipartimento di Ingegneria dell'Energia Elettrica e dell'Informazione "Guglielmo Marconi", Via dell'Università 50, Cesena, 47521 Italia
- ^{ag}Cadi Ayyad University, Physics Department, Faculty of Science Semlalia, Av. My Abdellah, P.O.B. 2390, Marrakech, 40000 Morocco
- ^{ah}Friedrich-Alexander-Universität Erlangen-Nürnberg (FAU), Erlangen Centre for Astroparticle Physics, Nikolaus-Fiebiger-Straße 2, 91058 Erlangen, Germany
- ^{ai}University of the Witwatersrand, School of Physics, Private Bag 3, Johannesburg, Wits 2050 South Africa
- ^{aj}Università di Catania, Dipartimento di Fisica e Astronomia "Ettore Majorana", Via Santa Sofia 64, Catania, 95123 Italy
- ^{ak}INFN, Sezione di Bari, via Orabona, 4, Bari, 70125 Italy
- ^{al}International Centre for Radio Astronomy Research, Curtin University, Bentley, WA 6102, Australia
- ^{am}University Würzburg, Emil-Fischer-Straße 31, Würzburg, 97074 Germany
- ^{an}Western Sydney University, School of Computing, Engineering and Mathematics, Locked Bag 1797, Penrith, NSW 2751 Australia
- ^{ao}IN2P3, LPC, Campus des Cézeaux 24, avenue des Landais BP 80026, Aubière Cedex, 63171 France
- ^{ap}Università di Genova, Via Dodecaneso 33, Genova, 16146 Italy
- ^{aq}University of Granada, Dpto. de Física Teórica y del Cosmos & C.A.F.P.E., 18071 Granada, Spain
- ^{ar}NIOZ (Royal Netherlands Institute for Sea Research), PO Box 59, Den Burg, Texel, 1790 AB, the Netherlands
- ^{as}Leiden University, Leiden Institute of Physics, PO Box 9504, Leiden, 2300 RA Netherlands
- ^{at}National Centre for Nuclear Research, 02-093 Warsaw, Poland
- ^{au}Tbilisi State University, Department of Physics, 3, Chavchavadze Ave., Tbilisi, 0179 Georgia
- ^{av}The University of Georgia, Institute of Physics, Kostava str. 77, Tbilisi, 0171 Georgia
- ^{aw}Institut Universitaire de France, 1 rue Descartes, Paris, 75005 France
- ^{ax}IN2P3, 3, Rue Michel-Ange, Paris 16, 75794 France
- ^{ay}LPC, Campus des Cézeaux 24, avenue des Landais BP 80026, Aubière Cedex, 63171 France
- ^{az}University of Johannesburg, Department Physics, PO Box 524, Auckland Park, 2006 South Africa
- ^{ba}Università degli Studi della Campania "Luigi Vanvitelli", CAPACITY, Laboratorio CIRCE - Dip. Di Matematica e Fisica - Viale Carlo III di Borbone 153, San Nicola La Strada, 81020 Italy
- ^{bb}Laboratoire Univers et Particules de Montpellier, Place Eugène Bataillon - CC 72, Montpellier Cédex 05, 34095 France
- ^{bc}Friedrich-Alexander-Universität Erlangen-Nürnberg (FAU), Remeis Sternwarte, Sternwartstraße 7, 96049 Bamberg, Germany
- ^{bd}Université de Haute Alsace, rue des Frères Lumière, 68093 Mulhouse Cedex, France
- ^{be}AstroCeNT, Nicolaus Copernicus Astronomical Center, Polish Academy of Sciences, Rektorska 4, Warsaw, 00-614 Poland

Acknowledgements

The authors acknowledge the financial support of the funding agencies: Agence Nationale de la Recherche (contract ANR-15-CE31-0020), Centre National de la Recherche Scientifique (CNRS), Commission Européenne (FEDER fund and Marie Curie Program), LabEx UnivEarthS (ANR-10-LABX-0023 and ANR-18-IDEX-0001), Paris Île-de-France Region, France; Shota Rustaveli National Science Foundation of Georgia (SRNSFG, FR-22-13708), Georgia; The General Secretariat of Research and Innovation (GSRI), Greece Istituto Nazionale di Fisica Nucleare (INFN), Ministero dell'Università e della Ricerca (MIUR), PRIN 2017 program (Grant NAT-NET 2017W4HA7S) Italy; Ministry of Higher Education, Scientific Research and Innovation, Morocco, and the Arab Fund for Economic and Social Development, Kuwait; Nederlandse organisatie voor Wetenschappelijk Onderzoek (NWO), the Netherlands; The National Science Centre, Poland (2021/41/N/ST2/01177); The grant "AstroCeNT: Particle Astrophysics Science and Technology Centre", carried out within the International Research Agendas programme of the Foundation for Polish Science financed by the European Union under the European Regional Development Fund; National Authority for Scientific Research (ANCS), Romania; Grants PID2021-124591NB-C41, -C42, -C43 funded by MCIN/AEI/ 10.13039/501100011033 and, as appropriate, by "ERDF A way of making Europe", by the "European Union" or by the "European Union NextGenerationEU/PRTR", Programa de Planes Complementarios I+D+I (refs. ASFAE/2022/023, ASFAE/2022/014), Programa Prometeo (PROMETEO/2020/019) and GenT (refs. CIDEAGENT/2018/034, /2019/043, /2020/049, /2021/23) of the Generalitat Valenciana, Junta de Andalucía (ref. SOMM17/6104/UGR, P18-FR-5057), EU: MSC program (ref. 101025085), Programa María Zambrano (Spanish Ministry of Universities, funded by the European Union, NextGenerationEU), Spain; The European Union's Horizon 2020 Research and Innovation Programme (ChETEC-INFRA - Project no. 101008324).